Journal of Science and Technology in Civil Engineering, HUCE, 2024, 18 (1): 12–23

EFFECT OF FIBER CONTENT ON FLEXURAL FRACTURE PARAMETERS OF HIGH-PERFORMANCE STEEL FIBER-REINFORCED CONCRETE

Thi-Ngoc-Han Vuong[a], Duy-Liem Nguyen[a,*], H. T. Tai Nguyen[a], Tri N. M. Nguyen[b]

[a]*Faculty of Civil Engineering, Ho Chi Minh City University of Technology and Education, 01 Vo Van Ngan street, Thu Duc city, Ho Chi Minh city, Vietnam*
[b]*Department of Civil Engineering, Industrial University of Ho Chi Minh City, 12 Nguyen Van Bao street, ward 4, Go Vap district, Ho Chi Minh city, Vietnam*

Article history:
Received 26/4/2023, Revised 14/3/2024, Accepted 20/3/2024

Abstract

This study deals with the effect of fiber content on fracture parameters of high-performance steel-fiber-reinforced concretes through a bending test program. All the high-performance steel-fiber-reinforced concretes flexural specimens were tested under configuration of three-point loading. The fracture parameters were hardening energy, softening energy and length of cohesive crack. Two steel fiber types were employed in the studied high-performance steel-fiber-reinforced concretes, including 35 mm long hooked fiber and 13 mm short smooth fiber. The high-performance steel-fiber-reinforced concretes were produced from the same matrix but added different fiber contents as follows: 0.0 vol.%, 0.5 vol.%, 1.0 vol.%, and 1.5 vol.%. The experimental results demonstrated that two parameters, including the hardening energy and softening energy, were observed to increase with increasing of fiber content, regardless of fiber type. The hardening energy was lower than the softening energy at any fiber content. The short smooth fibers generally produced the higher fracture energy parameters than the long hooked fibers. The highest total fracture energies of the high-performance steel-fiber-reinforced concretes were observed at 1.0 vol.% as follows: 58.25 kJ/m^2 for using short smooth and 59.16 kJ/m^2 for using long hooked fibers. Besides, the addition of reinforcing fibers considerably improved the length of the cohesive crack of the high-performance steel-fiber-reinforced concretes: from 0.58 mm using no fiber to 519.85 mm using short smooth fibers 0.5 vol.%.

Keywords: fracture energy; deflection-softening; deflection-hardening; cohesive crack; fiber content.

https://doi.org/10.31814/stce.huce2024-18(1)-02

1. Introduction

A lot of research has been reported various strategies to enhance the construction structure of civil and military infrastructures, with the aim of protecting human life under extreme loadings or corrosive environments [1–3]. High-performance steel-fiber-reinforced concretes (HPSFRCs) is known as a type of advanced material that can satisfy the demand for enhancing the structure's resistance as well as preventing the natural disasters [4–8]. This is because HPSFRCs exhibited many superior advantages, consisting of exceptional mechanical resistance, high energy absorption capacity, work-hardening behavior accompanying with numerous micro-cracks based on fiber bridging mechanism [7–11]. It is noted that HPSFRCs can be classified as an innovative concrete, in which sand is considered as a coarse aggregate whereas mineral admixtures such as silica fume or fly ash plays is considered as a fine aggregate [12]. The term of "concrete" called for high-performance cementitious composites have been popularly adopted [2, 4, 5, 7]. Adding steel fiber into the plain HPSFRC

*Corresponding author. *E-mail address:* liemnd@hcmute.edu.vn (Nguyen, D.-L.)

concrete has been a common strategy for enhancing the mechanical/physical properties of HPSFRCs [13–18]. In detail, Song and Hwang [13] investigated the mechanical properties of HPSFRCs with the steel fiber volume fraction of 0.5, 1.0, 1.5 and 2 vol.%. They declared that the compressive strength of 98 MPa could be achieved at 1.5 vol.% for the studied HPSRFCs. Nguyen et al. [14] studied the macro, meso and micro steel smooth fibers on tensile and characteristics of HPSFRCs. They found that the macro fibers produced the highest strength, strain capacity and toughness of HPSFRCs. Guo et al. [15] also stated that the fiber content of 150 kg/m^3 could decrease the moisture diffusion and accordingly the drying shrinkage, in addition to generating the minimum weight loss. The dynamic behavior of HPSFRCs was also significantly depended on steel fiber features [16]. Zemei et al. [17] investigated the mechanical properties of HPSFRCs using three shapes of steel fibers with four steel fiber volume fractions of 0.0, 1.0, 2.0, and 3.0 vol.%. They concluded that the increasing fiber content would gradually decrease the flowability. Qadir et al. [18] studied the effect of eight fiber volume fractions of 0.0, 1.0, 1.5, 2.0, 2.5, 3.0, 3.5, and 4.0 vol.% on the mechanical properties and fracture parameters of ultra high-performance steel-fiber-reinforced concrete (UHPFRC). They stated that the facture parameters of the UHPFRC increased with an increase of fiber volume content. Additionally, Tran et al. [19] studied the fracture parameters of UHPFRC by adding 1.0 and 1.5 vol.% steel fibers in mortar matrix. They declared that the smooth steel fibers had greater fracture strength and specific work-of fracture rates than the twisted fibers.

From the literature review mentioned above, the effect of various fiber characteristics on mechanical properties of HPSFRC has been investigated. However, the effect of fiber content on fracture parameters of HPSFRCs has been limited, this can be considered as a research gap required to fulfill. This research work is expected to provide helpful information on the effect of fiber content on flexural fracture parameters referring to experimental test in previous studies [20]. In addition, the better understanding flexural fracture mechanism of the HPSFRCs can be considered as a novelty of this study.

2. Parameters of fracture energy and crack propagation under bending

2.1. Parameters of fracture energy

Fig. 1 shows the typical bending stress – deflection ($f-\delta$) of HPSFRCs [21]. As observed in Fig. 1, the energy parameters are as follows:

- The hardening fracture energy (denoted by G_w) is the area under the flexural stress – deflection response curve from 0 to the post crack (point B) of deflection, as shown in Eq (1).

- The softening fracture energy (denoted by G_s) is the area bellow the flexural stress – deflection response curve from the post crack (MOR) to the end of extend line (point E) of deflection as show in as Eq. (2).

- Entire fracture energy was (denoted by G_{tt}) determined by total hardening fracture energy (G_{tt}) and softening fracture energy (G_{tt}), as displayed Eq. (3).

$$G_w = \int_{\varepsilon=0}^{\varepsilon=\varepsilon_{\mathrm{MOR}}} (f(\varepsilon)\, d(\varepsilon)) \times S = \int_{0}^{S\,\varepsilon_{\mathrm{MOR}}} f(S\,\varepsilon) d(S\,\varepsilon) = \int_{\delta=0}^{\delta=\delta_{\mathrm{MOR}}} f(\delta) d(\delta) \tag{1}$$

$$G_s = \int_{\varepsilon=\varepsilon_{\mathrm{MOR}}}^{\varepsilon=\varepsilon_e} (f(\varepsilon)\, d(\varepsilon)) \times S = \int_{\varepsilon_{\mathrm{MOR}} S}^{\varepsilon_e S} (f(\varepsilon S)\, d(\varepsilon S)) = \int_{\delta=\delta_{\mathrm{MOR}}}^{\delta=\delta_E} f(\delta) d(\delta) \tag{2}$$

$$G_{tt} = \sum G = G_w + G_S = \int_{\delta=0}^{\delta=\delta_{\mathrm{MOR}}} f(\delta) d(\delta) + \int_{\delta=\delta_{\mathrm{MOR}}}^{\delta=\delta_E} f(\delta) d(\delta) \tag{3}$$

where S is the span length, δ_{MOR} is the deflection at the post crack, δ_E is the deflection at the end of extend curve (point E).

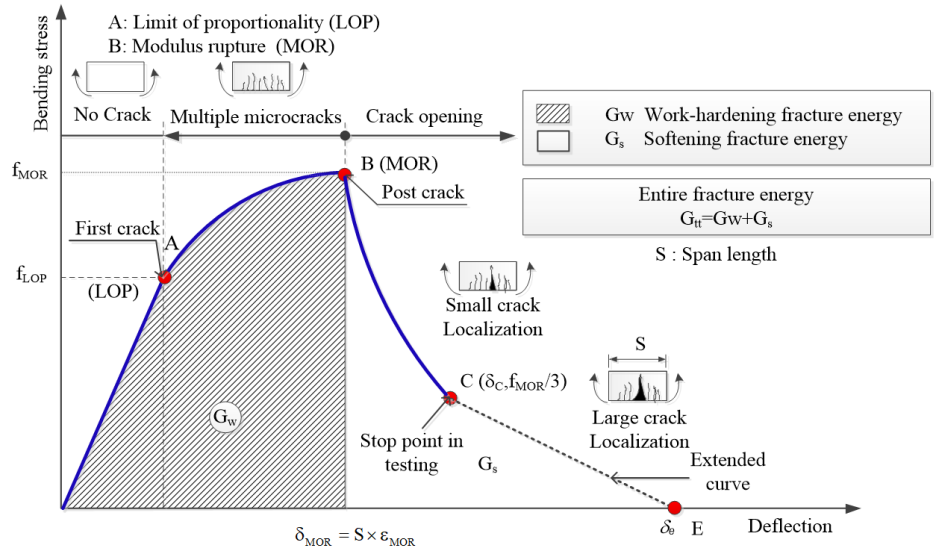

Figure 1. Typical strain-hardening response curve of HPSFRCs

2.2. *The length of cohesive crack*

The length of cohesive of HPSFRCs (L_{cz}) is the distance from the crack tip point (denoted point T), which has the critical crack opening width $w = w_c$ and its corresponding stress $f = 0$, to the point having crack width $w = 0$ and its corresponding stress of maximum tress $f_{MOR} = f$ as shown in Fig. 2 [21]. Eq. (4) mathematically displays the L_{cz} of HPSFRCs, which was mainly based on the bilinear model of stress versus crack opening developed by Hillerborg et al. [22, 23].

$$L_{cz} = \frac{EG_s}{(f_{MOR})^2} \tag{4}$$

where E is denoted the elastic modulus, f_{MOR} is denoted the flexural strength of HPSFRCs.

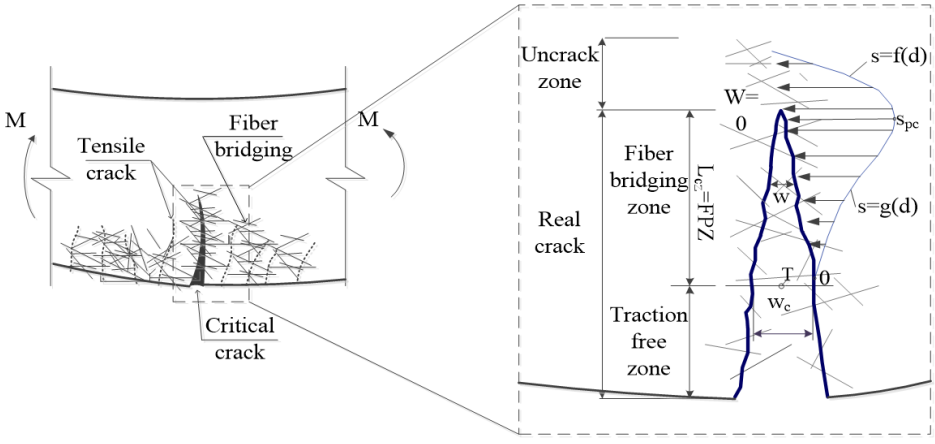

Figure 2. Cohesive crack length of HPSFRCs

3. Experimental program

An experimental program conducted in this investigation is displayed in Fig. 3. As can be seen from Fig. 3, there are two types of steel fibers, including short smooth (SS) and long hooked (LH)

fibers with different four volume contents added in the same HPSFRC mortar as follows: 0 vol.% (notated NF series), 0.5 vol.% (notated SS-0.5 series, LH-0.5 series), 1.0 vol.% (notated SS-1.0 series, LH-1.0 series), and 1.5%.vol (notated SS-1.5 series, LH-1.5 series).

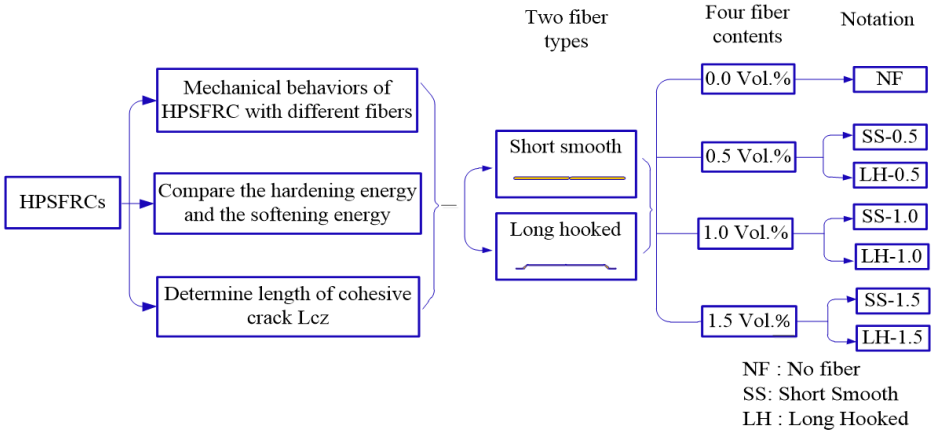

Figure 3. Experimental program

3.1. Materials used

The compositions of HPSFRC are presented in Table 1 while Table 2 provides the properties of the two fibers used in this study and their images are shown in Fig. 4. As can be presented in Table 2 and Fig. 4, the hooked steel fiber has a diameter of 0.5 mm and a length of 35 mm, while the straight smooth steel fiber has a diameter of 0.2 mm and a length of 13 mm. The two types of steel fibers had a density and elastic modulus of 7.9 g/cm^3 and 200 GPa, respectively. The tensile strength of the hooked steel fibers was 1200 MPa, while that of the straight smooth steel fibers was 2500 MPa [20].

Table 1. Composition of matrix mixture

Concrete	Cement (INSSE PC40) (kg/m^3)	Silica Fume (kg/m^3)	Sand (kg/m^3)	Fly Ash (kg/m^3)	Superplasticizer (kg/m^3)	Water (kg/m^3)
HPSFRC	810	71	1013	203	40	263

Table 2. Properties of fibers

Notation	Diameter (mm)	Length (mm)	Aspect ratio (L/D)	Tensile strength (MPa)
LH	0.5	35	70	1200
SS	0.2	13	65	2500

Table 3 presents the chemical and physical properties of fly ash, cement, and silica fume, including their information on fineness and specific gravity. Cement, silica fume, and fly ash have their fineness values of 348, 20,000, and 289 m^2/kg, respectively, while their specific gravities are 3.15, 2.24, and 2.41, respectively. Table 4 provides the characteristics of sand and superplasticizer used in this article. As provided in Table 4, the sand has its maximum diameters of 1 mm, density of 2.65 g/cm^3, and volumetric mass of 1.56 g/cm^3. The superplasticizer named Adva Cast 512 - W.R. Grace has chemical origin from Naphtalen Formadehyt Sulfonat and volumetric mass changing from 1.19 to 1.22 g/cm^3. It was remarked that the silica fume and fly ash in the HPSFRC admixture can work the role of fine

aggregates, whereas the sand can play the role of coarse aggregate due to its much greater particle size.

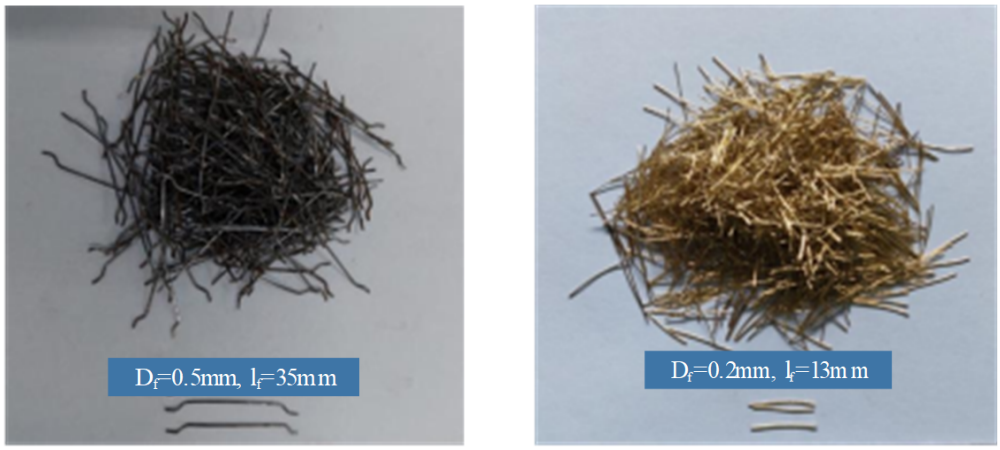

(a) Hooked steel fibers (b) Straight smooth steel fibers

Figure 4. Images of fibers

Table 3. Chemical and physical properties of fly ash, cement and silica fume

Materials			
Chemical and physical	Fly ash	Cement	Silica fume
SiO_2(%)	56.25	20.60	95.38
Al_2O_3 (%)	20.04	5.10	0.2
CaO (%)	1.90	62.6	0.13
MgO (%)	1.30	3.00	0.37
Fe_2O_3(%)	3.48	3.20	0.0063
SO_3(%)	0.58	3.60	-
$K_2O + Na_2O$ (%)	1.02	1.40	1.81
C (%)	-	-	0.007
Loss on ignition (%)	9.52	0.30	3.859
Fineness(m^2/kg)	289	348	20,000
Specific gravity	2.41	3.15	2.24

Table 4. Properties of sand and superplasticizer used

Properties	Sand	Superplasticizer
Name	-	Adva Cast 512 - W.R. Grace
Density (g/cm^3)	2.65	-
Volumetric mass (g/cm^3)	1.56	1.19 – 1.22
Maximum size of diameter (mm)	1.00	-
Chemical origin	-	Naphtalen Formadehyt Sulfonat

3.2. Specimen preparation

The mixing HPSFRC materials and specimen preparation were conducted in a laboratory of Ho Chi Minh City University of Technology and Education. Fig. 5 shows the mixing process and specimen preparation of the HPSFRCs. First, dry mixing of cement, sand, silica fume, and fly ash for about 10 minutes. Then, water is added and mixed for about 5 minutes. Next, superplasticizer is slowly added in batches to adjust the appropriate viscosity and mix evenly for about 10-15 minutes. Next, the steel fibers are gradually added by hand and mixed evenly for about 5-10 minutes, and the HPSFRC mixture containing fibers is poured into the mold, as shown in Fig. 5. After casting the specimens for 24 hours, all the specimens are cured in water at a temperature of 22-29°C for 14 days. Finally, all the bending specimens are taken out of the water and dried at room temperature in the laboratory before testing. At least three specimens were tested for each type of the HPSFRCs, and the average results were summarized and evaluated.

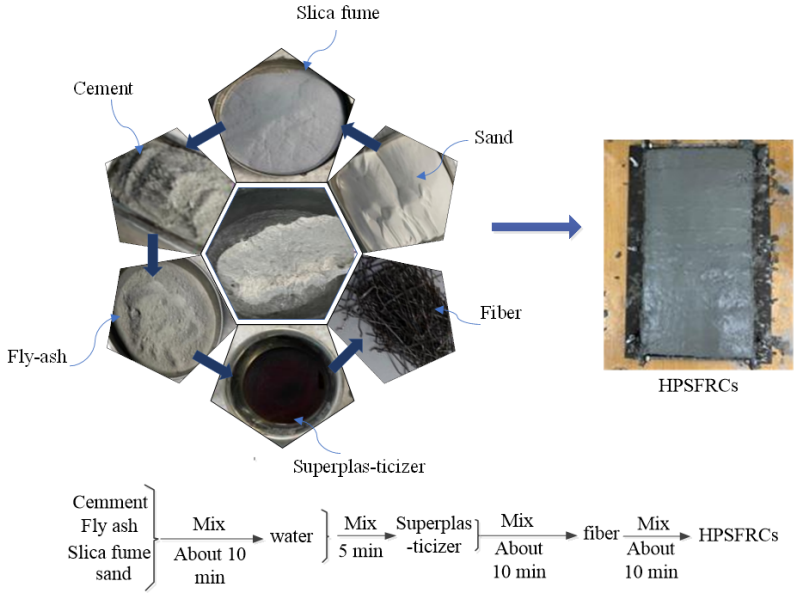

Figure 5. Mixing and specimen preparation

3.3. Experiment setup

Fig. 6 illustrates the experimental setup under three-point bending of the HPSFRCs. All specimens have the same prism-shaped with dimension of $40 \times 40 \times 160$ mm and their distance between the two supports in the three-point bending test was 120 mm. Although the HPSFRCs can be classified as a concrete, the small-sized specimen can be used for the HPSFRCs as a motar, which is performed according to Vietnamese standard TCVN 3121:2003 [24] due to the fine compositional materials with their particle size < 1 mm of the HPSFRCs. The tests were carried out using a Universal Testing Machine (UTM) with a loading capacity of 1000 kN. The data acquisition frequency was 1 Hz.

The maximum flexural strength (f_{MOR}) was determined according to Eq. (5):

$$f_{\mathrm{MOR}} = \frac{3}{2}\frac{P_{\max}L}{bh^2} \tag{5}$$

where, $P_{\max}$ is the maximum applied load, b and h are the width and height of the bending specimen, respectively, and L is the span length.

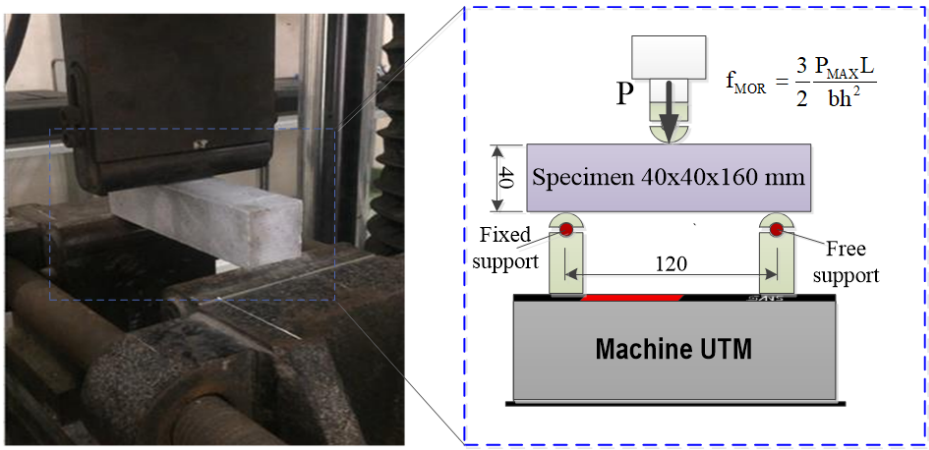

Figure 6. Photos of flexural test setups

4. Experiment result and discussion

4.1. Flexural strength versus behaviors of HPSFRCs

Fig. 7 displays the flexural stress (f) versus deflection (δ) responses of the HPSFRCs. Each HPSFRC series in Fig. 7 was performed with an outer general layout and an inner magnified response of the response curves. Three specimens of each HPSFRC series were tested.

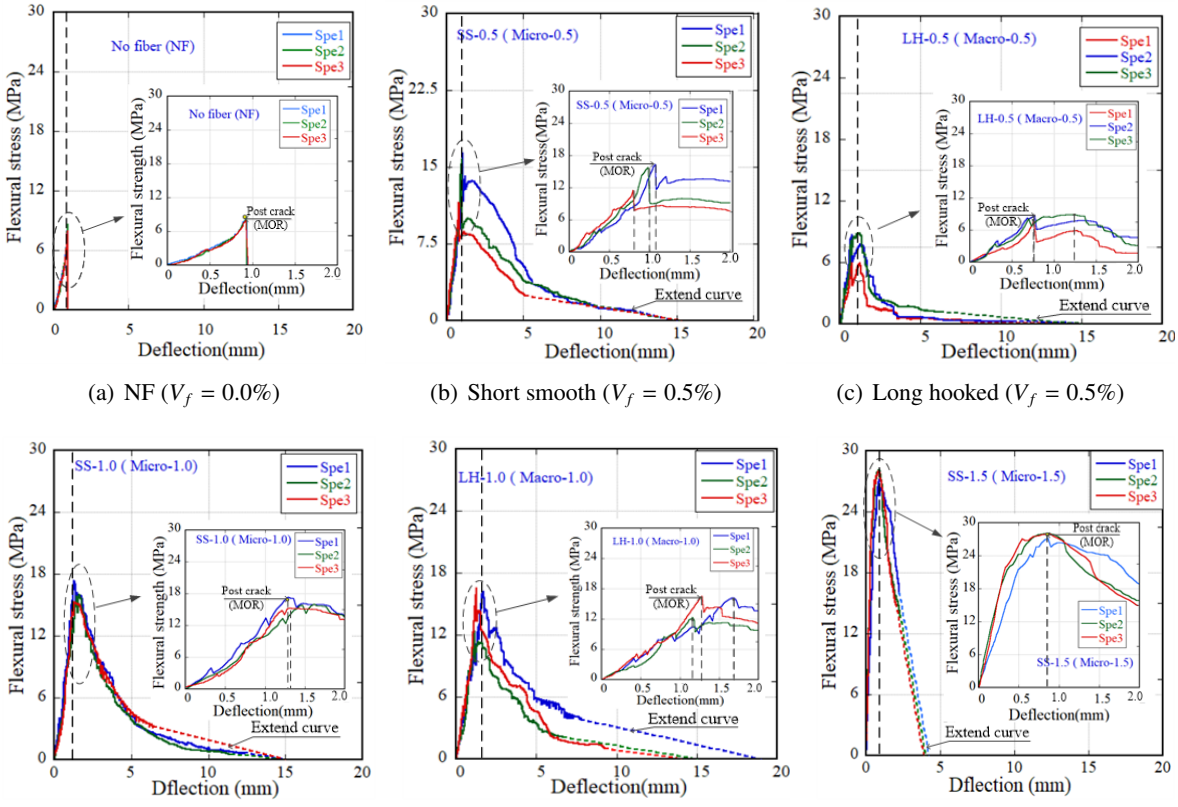

(a) NF (V_f = 0.0%) (b) Short smooth (V_f = 0.5%) (c) Long hooked (V_f = 0.5%)

(d) Short smooth (V_f = 1.0%) (e) Long hooked (V_f = 1.0%) (f) Short smooth (V_f = 1.5%)

4.2. Effect of steel fiber content on fracture energy

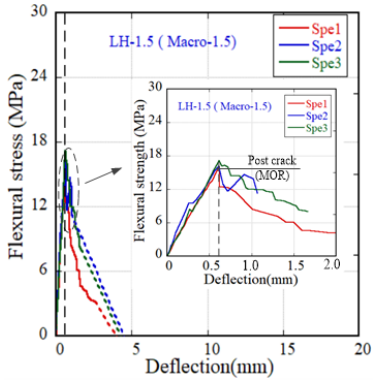

(g) Long hooked (V_f = 1.5%)

Figure 7. Flexural response of HPSFRCs

According to Eqs. (1), (2) and (3), the studied fracture energies, including the G_s, $G_w$and $G_{tt}$of all HPSFRC series were provided in Table 5, in addition to bending strength and deflection capacity of them. The comparative fracture energies of the HPSFRC is shown in Fig. 8. The work-hardening fracture energy (G_w) contributed slightly to the total fracture energy (G_{tt}), in a range of 3.97-15.85 kJ/m^2, regardless of the HPSFRCs containing fibers. The softening fracture energy (G_s) contributed considerably to the G_{tt}, in range of 13.88-50.13 kJ/m^2, i.e., from 73% to 90% of G_{tt}. As shown in Fig. 8, the G_w and G_s increased with increasing of SS fibers ranging from 0-1.5 vol.%. However, the G_w and G_s of HPSFRCs produced from LH fibers were optimal at 1.0 vol.%, i.e., the G_w and G_s decreased with the LH fiber more than 1.0 vol.%. The NF series produced the lowest G_w and G_s, the G_s from NF was negligible. The order of HPSFRC series in term of G_w was: SS-1.5 > SS-1.0 > LH-1.0 > SS-0.5 > LH-1.5 > LH-0.5 > NF, whereas the order of HPSFRC series in term of G_s was: LH-1.0 > SS-1.0 > SS-0.5 > SS-1.5 > LH-1.5 > LH-0.5 > NF. The highest G_{tt} were observed at 1.0 vol.% for both SS and LH fibers.

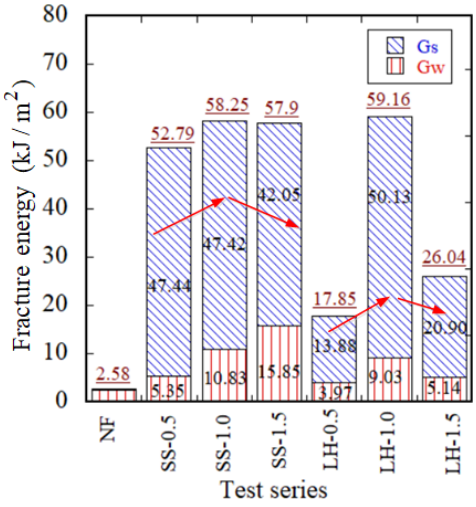

Figure 8. Energy behaviors of HPSFRC under bending

4.3. Effect of steel fiber content on cohesive crack length

Table 6 shows the elastic modulus and cohesive crack length of the HPSFRCs. The elastic modulus of the HPSFRCs were averaged to be from 896.32 MPa to 4155.17 MPa. The comparative length of cohesive cracks (L_{cz}) under bending of the HPSFRCs are graphically presented in Fig. 9, changing from 152.95 mm to 519.85 mm. This means there were the significant enhancements of L_{cz} with the additions of reinforcing fibers into HPSFRC matrix, since the L_{cz} value of NF series with no fiber was only 0.58 mm. As can be seen in Fig. 9, the SS-0.5 generated the highest L_{cz} whereas the NF created the lowest L_{cz}. Compared to the long hooked fibers, the short smooth fibers produced slightly smaller L_{cz} at 1.0 vol.% (0.91 times) and 1.5 vol.% (0.93 times), but notably greater at 0.5 vol.% (3.4 times). The order of HPSFRC series in term of L_{cz} was: SS-0.5 > LH-1.0 > SS-1.0 > LH-1.5 > SS-1.5 > LH-0.5 > NF.

Table 5. Flexural parameters and energy fracture of HPSFRC

Test Series	Specimen name	δ mm	f_t MPa	G_w kJ/m^2	G_s kJ/m^2	G_{tt} kJ/m^2	G_s/G_{tt}
NF	Spe1	0.94	7.95	2.63	0.00	2.63	
	Spe2	0.93	8.63	2.62	0.00	2.62	
	Spe3	0.92	7.93	2.49	0.12	2.61	
	Average	0.93	8.17	2.58	0.04	2.62	0.015
	Deviation	0.01	0.40	0.08	0.07	0.15	
SS-0.5	Spe1	1.07	16.37	6.36	58.04	64.41	
	Spe2	0.98	15.72	5.53	46.20	51.74	
	Spe3	0.79	11.50	4.16	38.07	42.24	
	Average	0.95	14.53	5.35	47.44	52.79	0.90
	Deviation	0.14	2.64	1.11	10.04	11.12	
SS-1.0	Spe1	1.29	17.33	10.38	49.29	59.67	
	Spe2	1.62	16.03	13.48	38.90	52.38	
	Spe3	1.31	15.30	8.62	54.08	62.70	
	Average	1.41	16.22	10.83	47.42	58.25	0.81
	Deviation	0.19	1.03	2.46	7.76	5.31	
SS-1.5	Spe1	0.86	27.17	14.35	47.06	61.41	
	Spe2	0.85	28.13	15.85	40.62	56.47	
	Spe3	0.86	27.98	17.34	38.46	55.80	
	Average	0.86	27.76	15.85	42.05	57.90	0.73
	Deviation	0.01	0.52	1.50	4.47	3.06	
LH-0.5	Spe1	0.76	7.79	2.08	9.20	11.28	
	Spe2	0.77	9.42	3.20	15.07	18.28	
	Spe3	0.70	9.53	6.62	17.36	23.99	
	Average	0.74	8.91	3.97	13.88	17.85	0.78
	Deviation	0.04	0.97	2.37	4.21	6.36	
LH-1.0	Spe1	1.66	16.17	12.60	67.94	80.54	
	Spe2	1.16	12.32	5.78	40.15	45.93	
	Spe3	1.28	16.51	8.71	42.31	51.02	
	Average	1.37	15.00	9.03	50.13	59.16	0.85
	Deviation	0.26	2.33	3.42	15.46	18.69	
LH-1.5	Spe1	0.62	15.93	5.10	14.44	19.54	
	Spe2	0.61	16.15	5.62	25.47	31.09	
	Spe3	0.61	17.16	4.69	22.80	27.50	
	Average	0.61	16.41	5.14	20.90	26.04	0.80
	Deviation	0.00	0.65	0.47	5.76	5.91	

In general, compared with the NF series with no fiber, the HPSFRCs containing the reinforcing fibers produced clear enhancements in fracture energies, although their enhancements were rather different. These enhancements can be explained due to interfacial debonding between the steel fiber and

Table 6. Elastic modulus and cohesive crack length of HPSFRCs

Test series	Elastic modulus, E (MPa)	Length of the cohesive crack, L_{cz} (mm)
NF	934.92	0.58
SS-0.5	2272.10	519.85
SS-1.0	1396.57	257.35
SS-1.5	4155.17	226.88
LH-0.5	896.32	152.95
LH-1.0	1277.12	284.44
LH-1.5	3144.65	243.77

mortar matrix [25, 26]. Besides, the fiber characteristics, including fiber geometry, quantity, and air bubble, can have an effect on the flexural fracture parameters. Fig. 10 shows the various distributions of short smooth and long hooked fibers added to the HPSFRC mixture. As can be seen from Fig. 10, the short smooth fibers with the volume content of a single type of fiber reinforcement produced more fiber number compared to that of long hooked fibers, resulting in a better bond between the fiber and air bubble at a failure crack. Obviously, when fiber volume content increases, its denser distribution also increases. So, the fracture energies of the HPSFRCs increase with increasing fiber content.

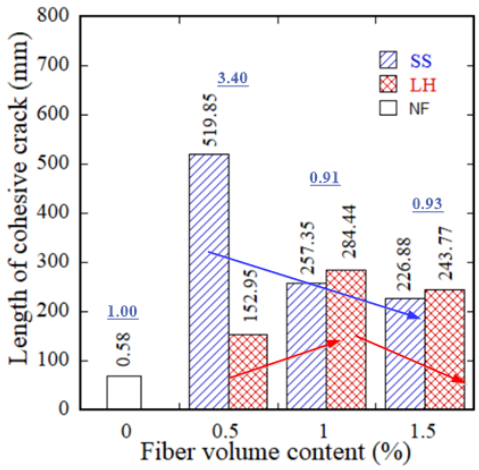

Figure 9. Length of cohesive crack of HPSFRCs under bending

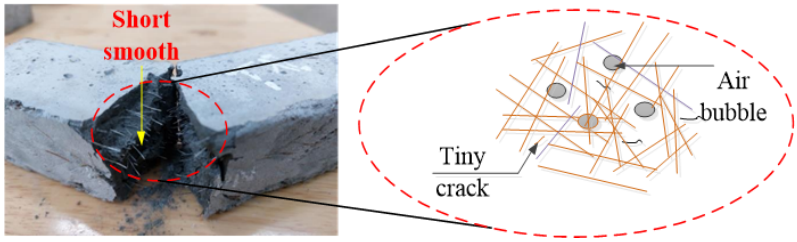

(a) Short smooth fiber

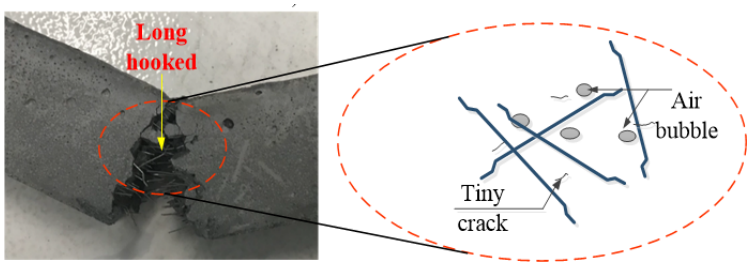

(b) Long hooked

Figure 10. Distribution of short smooth and long hooked fibers

5. Conclusions

The experimental results supplied helpful information on the influence of fiber content on flexural fracture parameters of the HPSFRCs. The main observations and conclusions can be listed as follows:

- The HPSFRC with no fiber exhibited a very low hardening fracture energy (2.58 kJ/m^2) and a negligible softening fracture energy. The adding steel fiber in the plain HPSFRC enhanced the hardening fracture energy up to 15.58 kJ/m^2 for the use of 1.5 vol.% short smooth fibers, and enhanced softening fracture energy up to 50.13 kJ/m^2 for the use of 1.0 vol.% long hooked fibers.

- The short smooth fibers generally produced the higher fracture energy parameters of the HPSFRCs than the long hooked fibers. At 1.0 vol.% fibers added, the highest total fracture energy of the HPSFRCs were achieved: 58.25 kJ/m^2 for using short smooth and 59.16 kJ/m^2 for using long hooked fibers.

- The hardening fracture energy was lower than the softening fracture energy for both of the studied fibers with their fractions ranging from 0.5 to 1.5 vol.%.

- For short smooth fibers, the hardening fracture energy and softening fracture energy increased with increasing of ranging from 0 to 1.5 vol.%. However, for the long hooked fibers, the highest hardening and softening fracture energy were observed at 1.0 vol.%.

- The plain HPSFRC with no fiber revealed the low cohesive crack length of 0.58 mm, wheres the HPSFRCs with reinforcing fibers exhibited the high cohesive crack lengths as follows: 152.95 mm for the use of 0.5 vol.% long hooked fibers and 519.85 mm for the use of 0.5 vol.% short smooth fibers.

Acknowledgements

This work belongs to the project grant No: T2023-152 funded by Ho Chi Minh City University of Technology and Education, Vietnam.

References

[1] Eskew, E., Jang, S. (2012). *Impacts and analysis for buildings under terrorist attacks*.

[2] Fehling, E., Schmidt, M., Stürwald, S. (2008). *Ultra High Performance Concrete (UHPC)*, volume 10. Proceedings of the International Symposium on Ultra-High Performance Concrete, Structural Materials and Engineering, series no. 10, Kassel, Germany.

[3] Li, Y., Zhang, L., Ma, C., Li, B., Zhu, J. (2020). Damage Mechanism of Mineral Admixture Concrete under Marine Corrosion and Freezing-Thawing Environment. *Advances in Civil Engineering*, 2020:1–13.

[4] Nunes, S., Pimentel, M., Sousa, C. (2021). Mechanical and Fracture Behaviour of an HPFRC. In *Fibre Reinforced Concrete: Improvements and Innovations II*, Springer International Publishing, 174–185.

[5] Song, J., Nguyen, D. L., Manathamsombat, C., Kim, D. J. (2015). Effect of fiber volume content on electromechanical behavior of strain-hardening steel-fiber-reinforced cementitious composites. *Journal of Composite Materials*, 49(29):3621–3634.

[6] Mishra, S., Sharma, H. K. (2018). Impact Resistance and Mechanical Properties of UHPFRC. *Iranian Journal of Science and Technology, Transactions of Civil Engineering*, 43(3):371–380.

[7] Afroughsabet, V., Biolzi, L., Ozbakkaloglu, T. (2016). High-performance fiber-reinforced concrete: a review. *Journal of Materials Science*, 51(14):6517–6551.

[8] Nguyen, D. L., Song, J., Manathamsombat, C., Kim, D. J. (2015). Comparative electromechanical damage-sensing behaviors of six strain-hardening steel fiber-reinforced cementitious composites under direct tension. *Composites Part B: Engineering*, 69:159–168.

[9] Özalp, F., Yilmaz, H. D., Akcay, B. (2022). Mechanical properties and impact resistance of concrete composites with hybrid steel fibers. *Frontiers of Structural and Civil Engineering*, 16(5):615–623.

[10] Liem, N. D., Ngo, T.-T., Phan, T.-D., Lai, T.-T., Le, D.-V. (2022). Predicting tensile properties of strain-hardening concretes containing hybrid fibers from single fiber pullout resistance. *Journal of Science and Technology in Civil Engineering (STCE) - HUCE*, 16(3):84–96.

[11] Hoan, P. T., Thuong, N. T. (2019). Shear resistance of ultra-high-performance concrete reinforced with hybrid steel fiber subjected to impact loading. *Journal of Science and Technology in Civil Engineering (STCE) - NUCE*, 13(1):12–20.

[12] Nguyen, D.-L., Thai, D.-K., Lam, M. N.-T. (2022). Synergy in Flexure of High-Performance Fiber-Reinforced Concrete with Hybrid Steel Fibers. *Journal of Materials in Civil Engineering*, 34(6).

[13] Song, P. S., Hwang, S. (2004). Mechanical properties of high-strength steel fiber-reinforced concrete. *Construction and Building Materials*, 18(9):669–673.

[14] Nguyen, D.-L., Nguyen, T.-Q., Nguyen, H.-T.-T. (2020). Influence of fiber size on mechanical properties of strain-hardening fiber-reinforced concrete. *Journal of Science and Technology in Civil Engineering (STCE) - NUCE*, 14(3):84–95.

[15] Guo, W., Zhang, P., Tian, Y., Wang, B., Ma, W. (2020). Influence of the Amount of Steel Fibers on Fracture Energy and Drying Shrinkage of HPFRCC. *Advances in Materials Science and Engineering*, 2020:1–15.

[16] Kesner, K. E., Billington, S. L., Douglas, K. S. (2003). Cyclic Response of Highly Ductile Fiber-Reinforced Cement-Based Composites. *ACI Materials Journal*, 100(5):381–390.

[17] Wu, Z., Shi, C., He, W., Wu, L. (2016). Effects of steel fiber content and shape on mechanical properties of ultra high performance concrete. *Construction and Building Materials*, 103:8–14.

[18] Qadir, H. H., Faraj, R. H., Sherwani, A. F. H., Mohammed, B. H., Younis, K. H. (2020). Mechanical properties and fracture parameters of ultra high performance steel fiber reinforced concrete composites made with extremely low water per binder ratios. *SN Applied Sciences*, 2(9).

[19] Tran, N. T., Tran, T. K., Jeon, J. K., Park, J. K., Kim, D. J. (2016). Fracture energy of ultra-high-performance fiber-reinforced concrete at high strain rates. *Cement and Concrete Research*, 79:169–184.

[20] Vuong, T. N. H., Nguyen, H. T. T., Nguyen, D. L. (2023). Influence of steel fiber content on bending resistance of high-performance fiber-reinforced concrete. In *Proceedings of the 11th National Conference on Mechanics: Solid Mechanics*, volume 1, 14–23.

[21] Nguyen, D.-L., Le, H.-V., Vu, T.-B.-N., Nguyen, V.-T., Tran, N.-T. (2023). Evaluating fracture characteristics of ultra-high-performance fiber-reinforced concrete in flexure and tension with size impact. *Construction and Building Materials*, 382:131224.

[22] Hillerborg, A., Modéer, M., Petersson, P.-E. (1976). Analysis of crack formation and crack growth in concrete by means of fracture mechanics and finite elements. *Cement and Concrete Research*, 6(6): 773–781.

[23] Hillerborg, A. (1985). The theoretical basis of a method to determine the fracture energy G_F of concrete. *Materials and Structures*, 18(4):291–296.

[24] TCVN 3121:2003. *Mortar for masonry - Test methods*.

[25] Yoo, D.-Y., Park, J.-J., Kim, S.-W. (2017). Fiber pullout behavior of HPFRCC: Effects of matrix strength and fiber type. *Composite Structures*, 174:263–276.

[26] Park, J. K., Ngo, T. T., Kim, D. J. (2019). Interfacial bond characteristics of steel fibers embedded in cementitious composites at high rates. *Cement and Concrete Research*, 123:105802.